Supplemental Table: Baseline characteristics of the finally included patients and examinations

Features	Measures
Patients	***n*=34**
Age	54.3±12.7 (27-81)
Sex	
Male	18 (52.9%)
Female	16 (47.1%)
Grade	
III	10 (29.4%)
Anaplastic astrocytoma	4
Anaplastic astrocytoma with molecular features of glioblastoma	1
Anaplastic oligodendroglioma	3
Anaplastic pilocytic astrocytoma	1
Anaplastic ependymoma	1
IV	24 (70.6%)
Glioblastoma	23
Diffuse midline glioma	1
Examination times per patient	
Once	26
Twice	5
Thrice	3
Examinations	***n*=45**
Interval after previous operation	
Shorter than 6 months	15 (33.3%)
6-12 months	12 (26.7%)
Longer than 12 months	18 (40.0%)
Location of the lesion of interest	
Convexity	27 (60.0%)
Deep	9 (20.0%)
Skull base	9 (20.0%)
Susceptibility effects by location	
Negligible	33 (73.3%)
Mild	11 (24.4%)
Considerable	1 (2.2%)
Susceptibility effects by hemorrhage	
Negligible	4 (8.9%)
Marginal	35 (77.8%)
Considerable	6 (13.3%)
Visualization grade on T1-PWI	
Grade 3	41 (91.1%)
Grade 2	4 (8.9%)
Grade 1	0 (0%)
Grade 0	0 (0%)
Visualization grade on T2*-PWI	
Grade 3	13 (28.9%)
Grade 2	23 (51.1%)
Grade 1	8 (17.8%)
Grade 0	1 (2.2%)

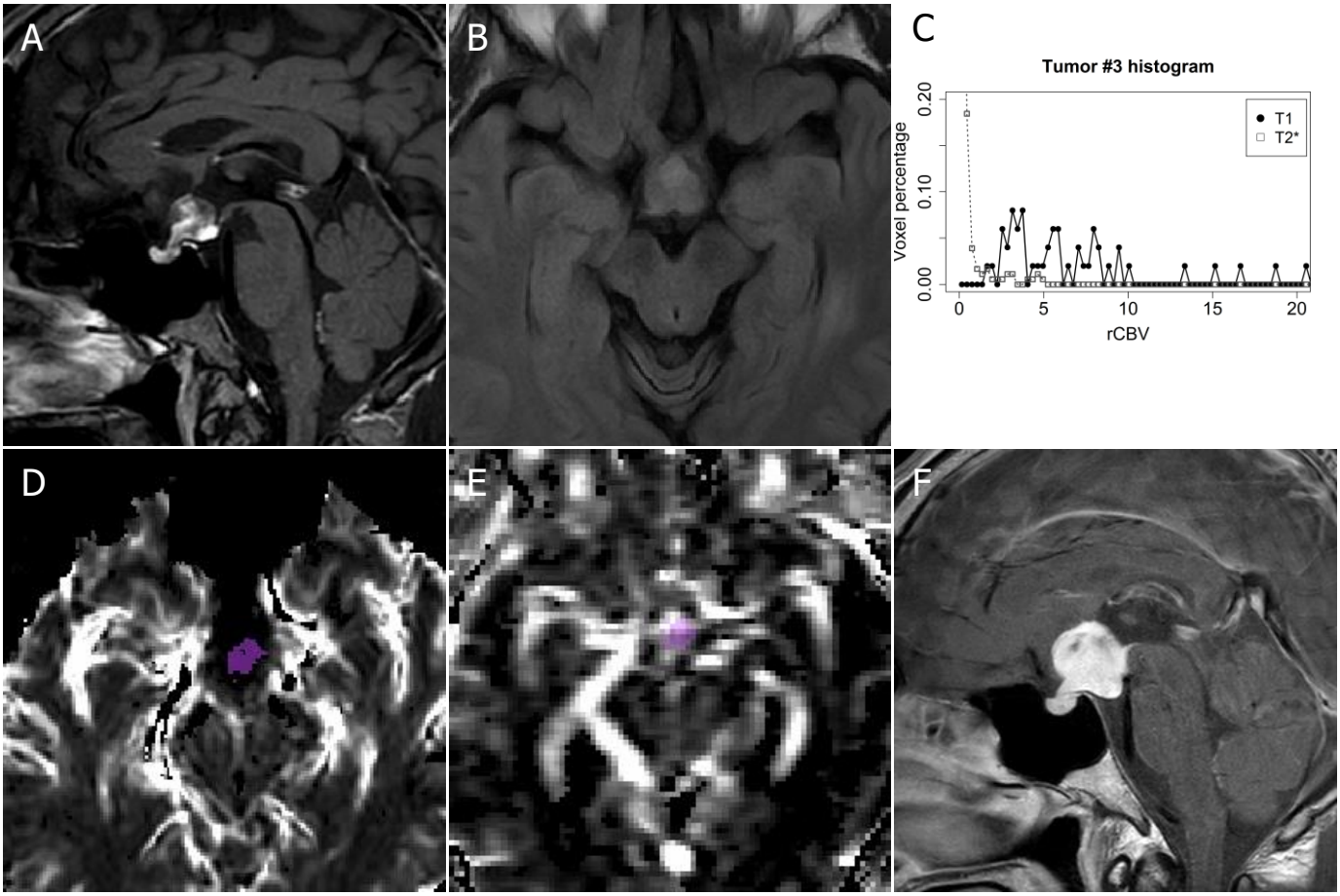

Supplemental FIG 1. A 31-year-old male who received surgical resection 2 years ago. A small enhancing mass was suspected in the suprasellar area (A, B). The T2*-PWI shows that the lesion is totally obscured due to SSE (D, rCBV 90th percentile 1.12) with grade 0 visualization. The leftmost peak of near-zero voxels is also seen on T2*-rCBV histogram (C). In contrast, the lesion is clearly visible (grade 3) on T1-PWI (E, rCBV 90th percentile 15.15). The purple-shaded area depicts the lesion mask, which was drawn on CE-T1WI (A). The lesion showed enlargement on the 2-month follow-up examination (F), and the patient underwent reoperation for confirmation as recurrent glioblastoma (progression group).

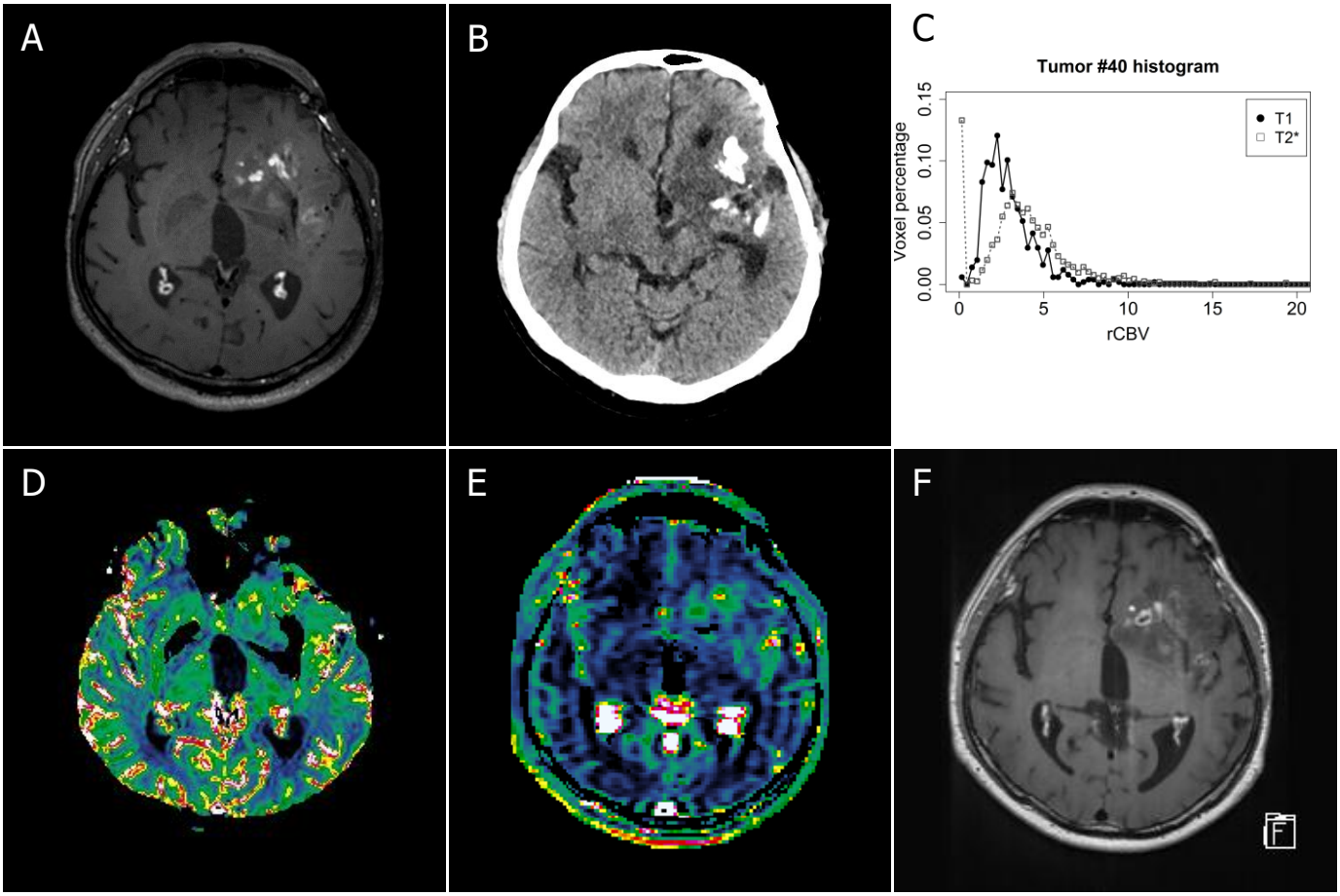

Supplemental FIG 2. A 53-year-old male, 8 years after the surgery of glioblastoma with oligodendroglioma component. The calcified mass at the left insular base is disturbed by susceptibility effects (A, B), with the leftmost peak of near-zero voxels on the histogram (C) and partial signal loss (grade 2) on T2*-PWI (D, rCBV 90th percentile 6.80, higher than cutoff). The lesion is more clearly visualized (grade 3) on the T1-PWI (E, rCBV 90th percentile 4.79, lower than cutoff). The mass was stable on the follow-up image 1 year later (F, nonprogression group).

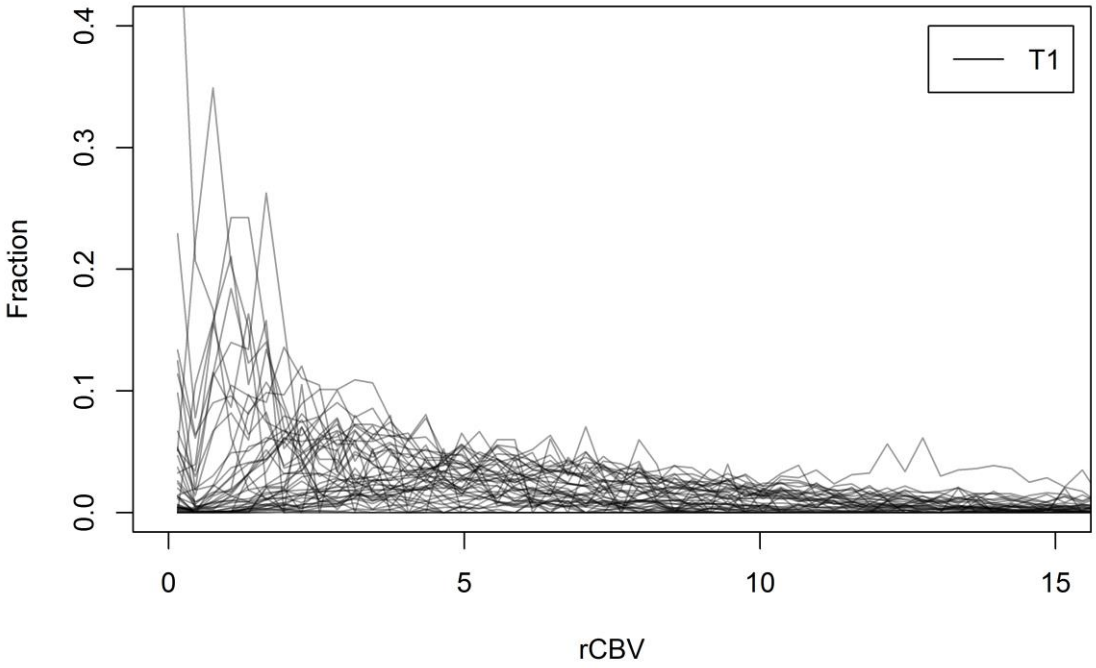

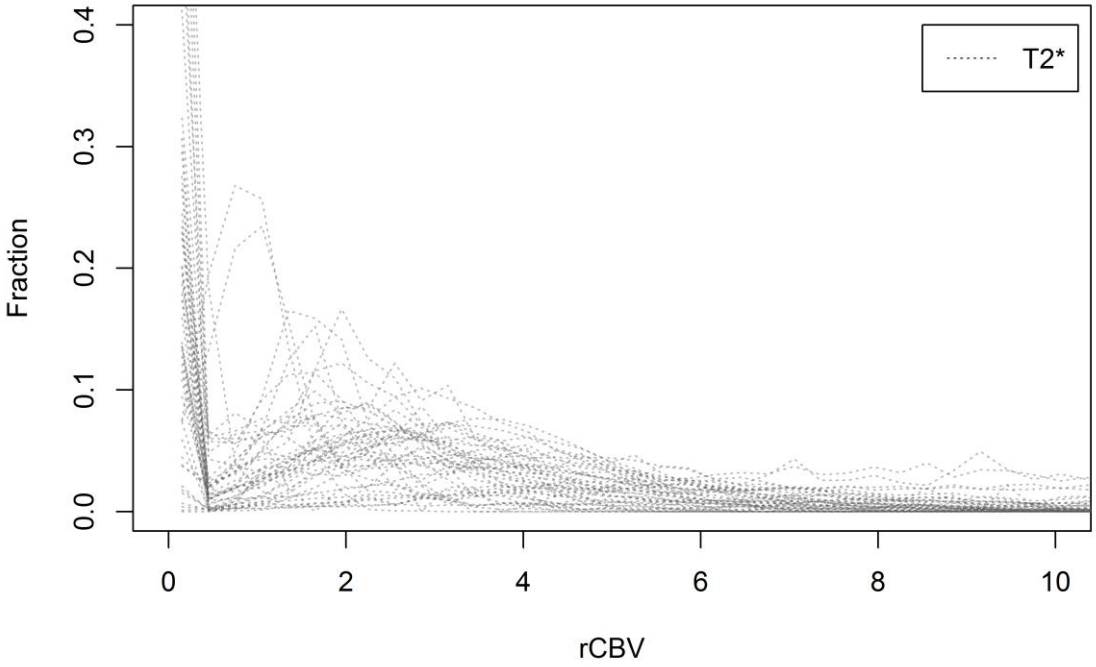

Supplemental FIG 3. Noncumulative histogram of T1- and T2*-rCBV values in all included examinations. T2*-rCBV (B) shows the leftmost clustered peak of near-zero lower outlier voxels, while the histogram of T1-rCBV (A) does not.

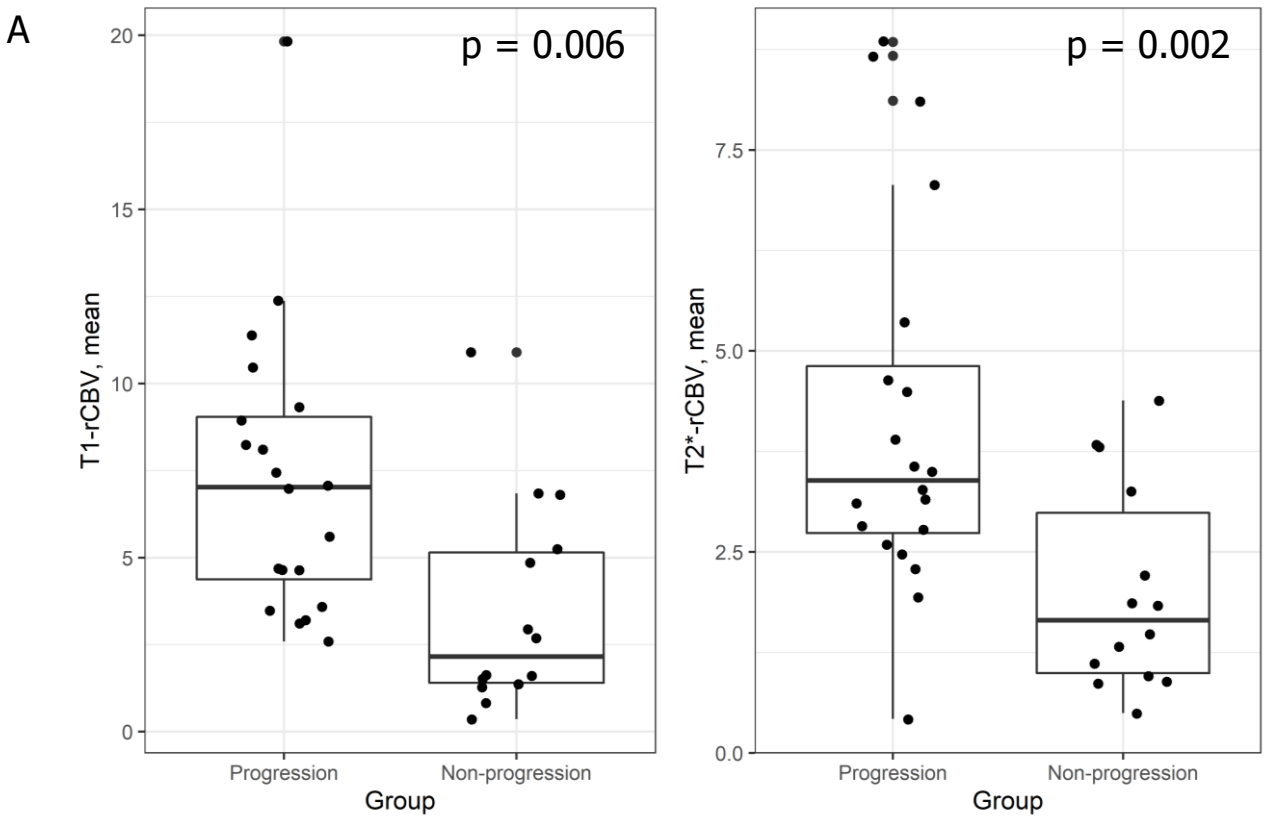

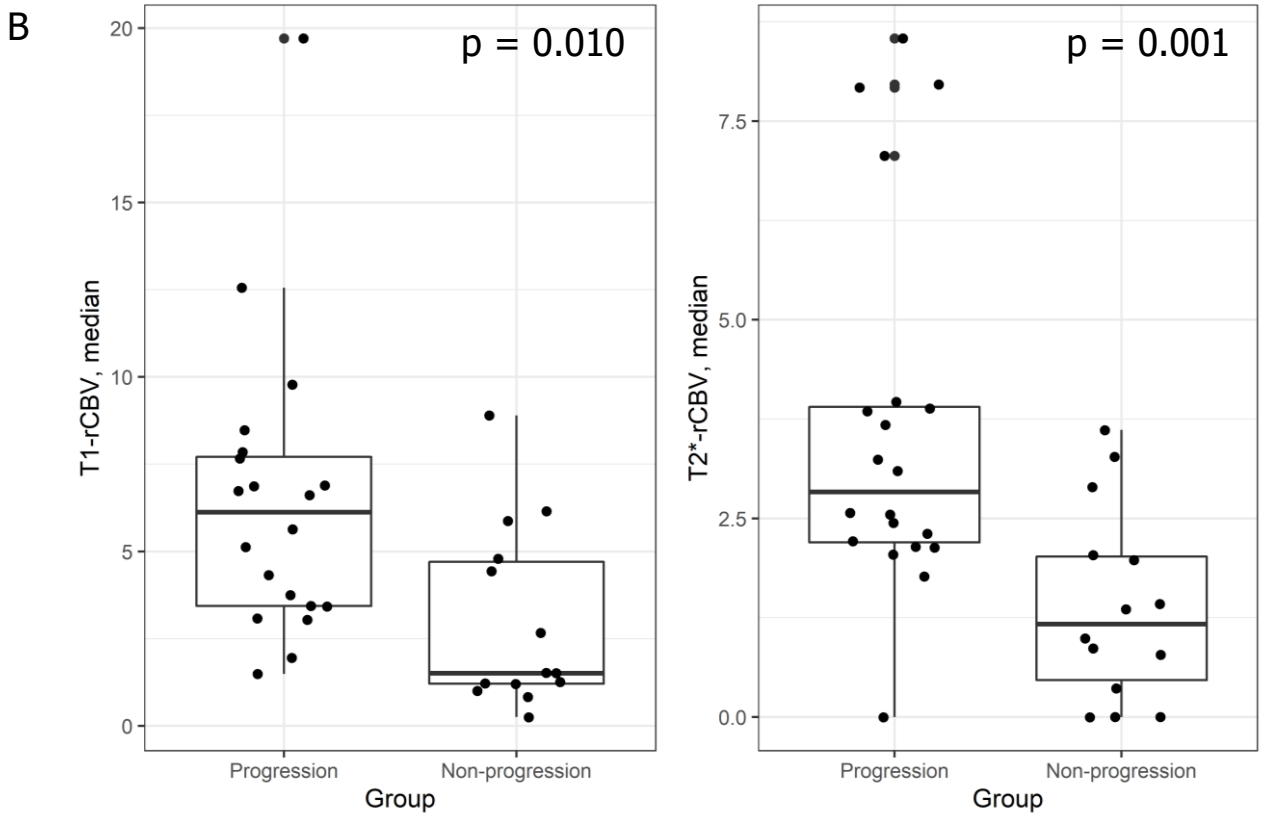

Supplemental FIG 4. (continued on the next page)

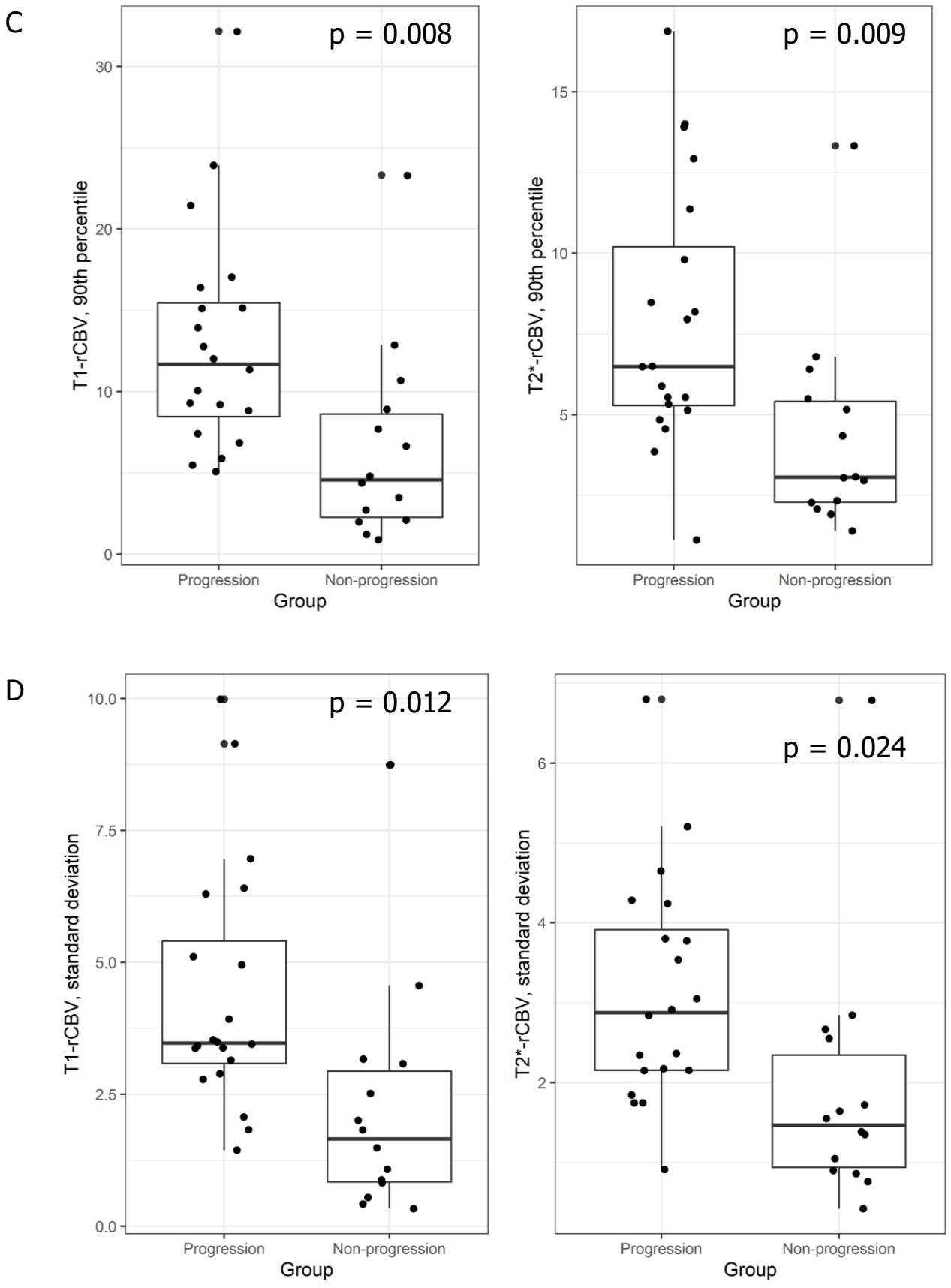

Supplemental FIG 4. Box plots displaying T1- and T2*-rCBV comparison of progression and nonprogression groups. Mean (A), median (B), 90th percentile (C), and standard deviation (D) values are shown. All rCBV values showed significant difference between the two groups.

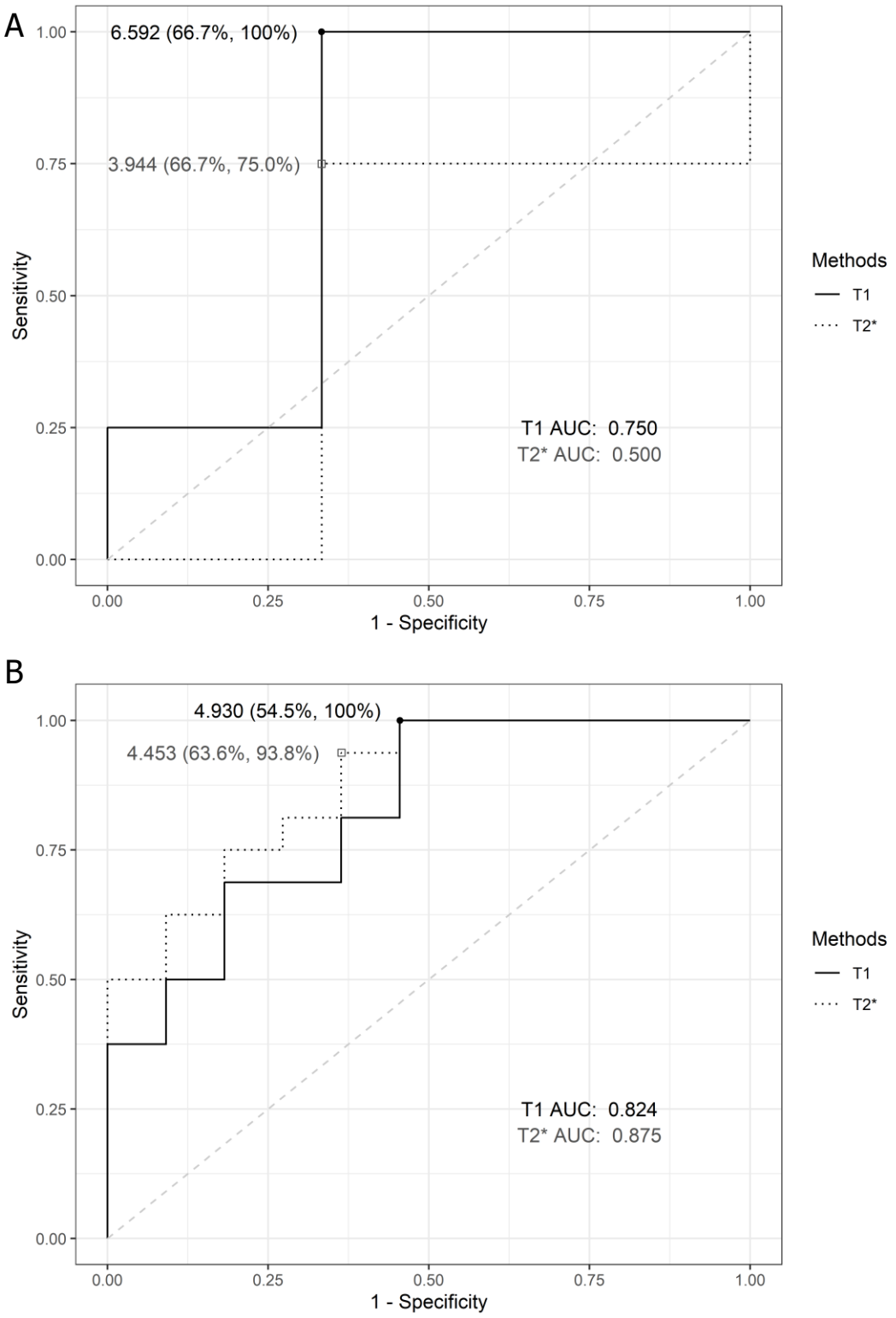

Supplemental FIG 5. The ROC curves of the 90th percentiles of T1- and T2*-rCBV values in the subgroups with SSE (less than 50% T2*-PWI visualization, A) and without SSE (more than 50% T2*-PWI visualization, B). The AUC value of T2*-PWI was lower than T1-PWI in the lesions with SSE (although not statistically significant, *P*=.117). On the other hand, AUC of T2*-PWI was comparable to T1-PWI among the lesions which were relatively well-visualized on T2*-PWI (*P*=.597).

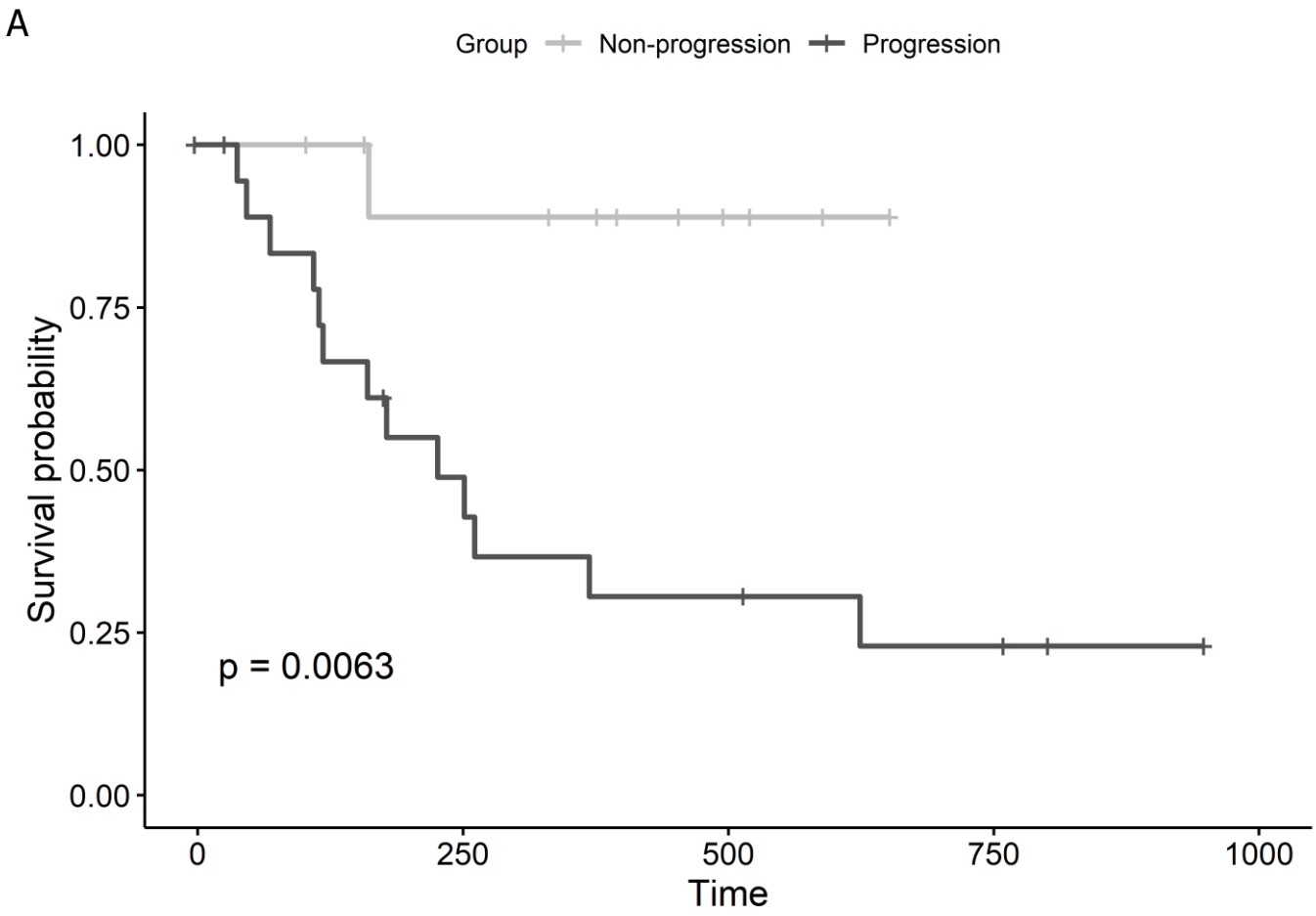

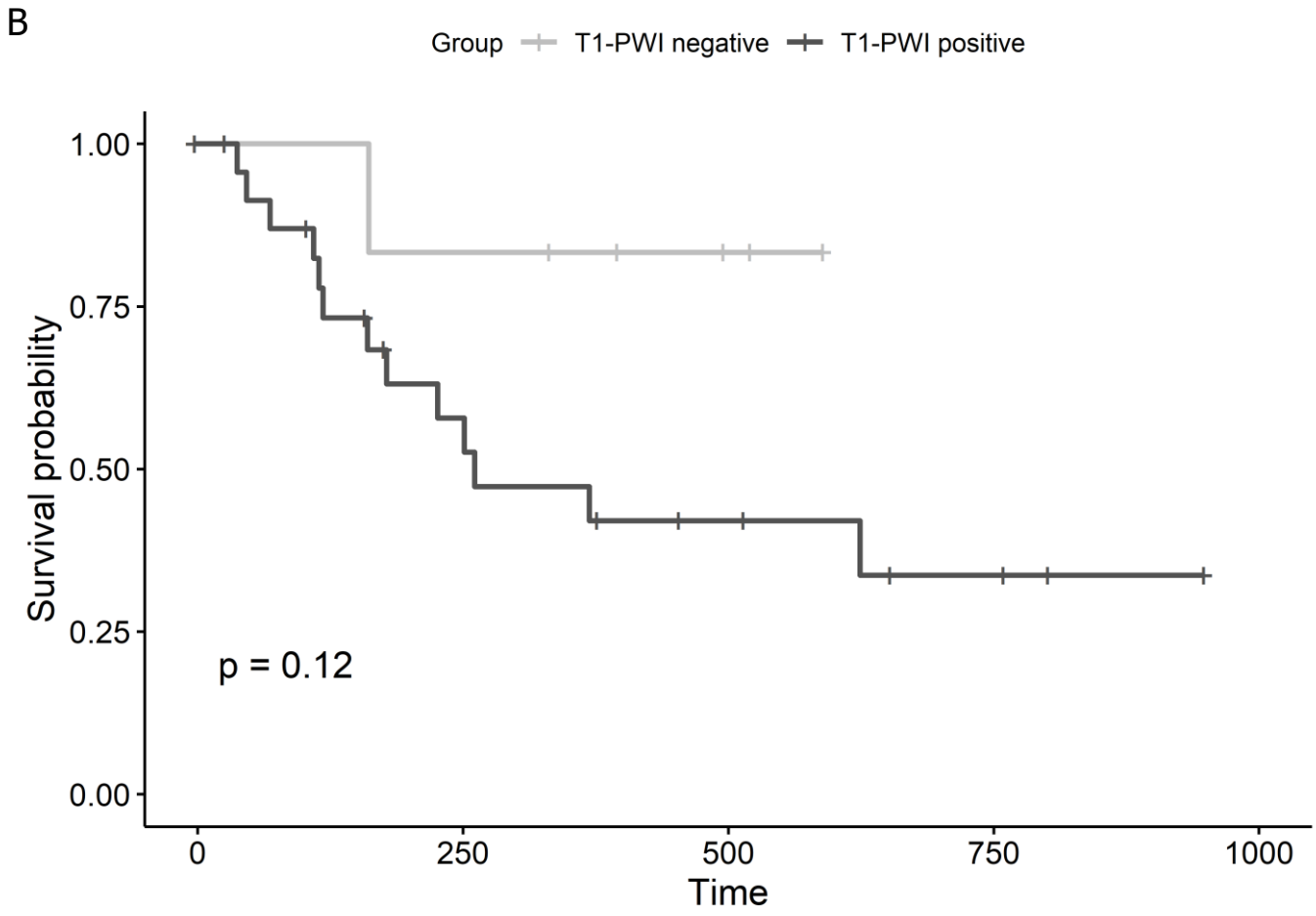

Supplemental FIG 6. (continued on the next page)

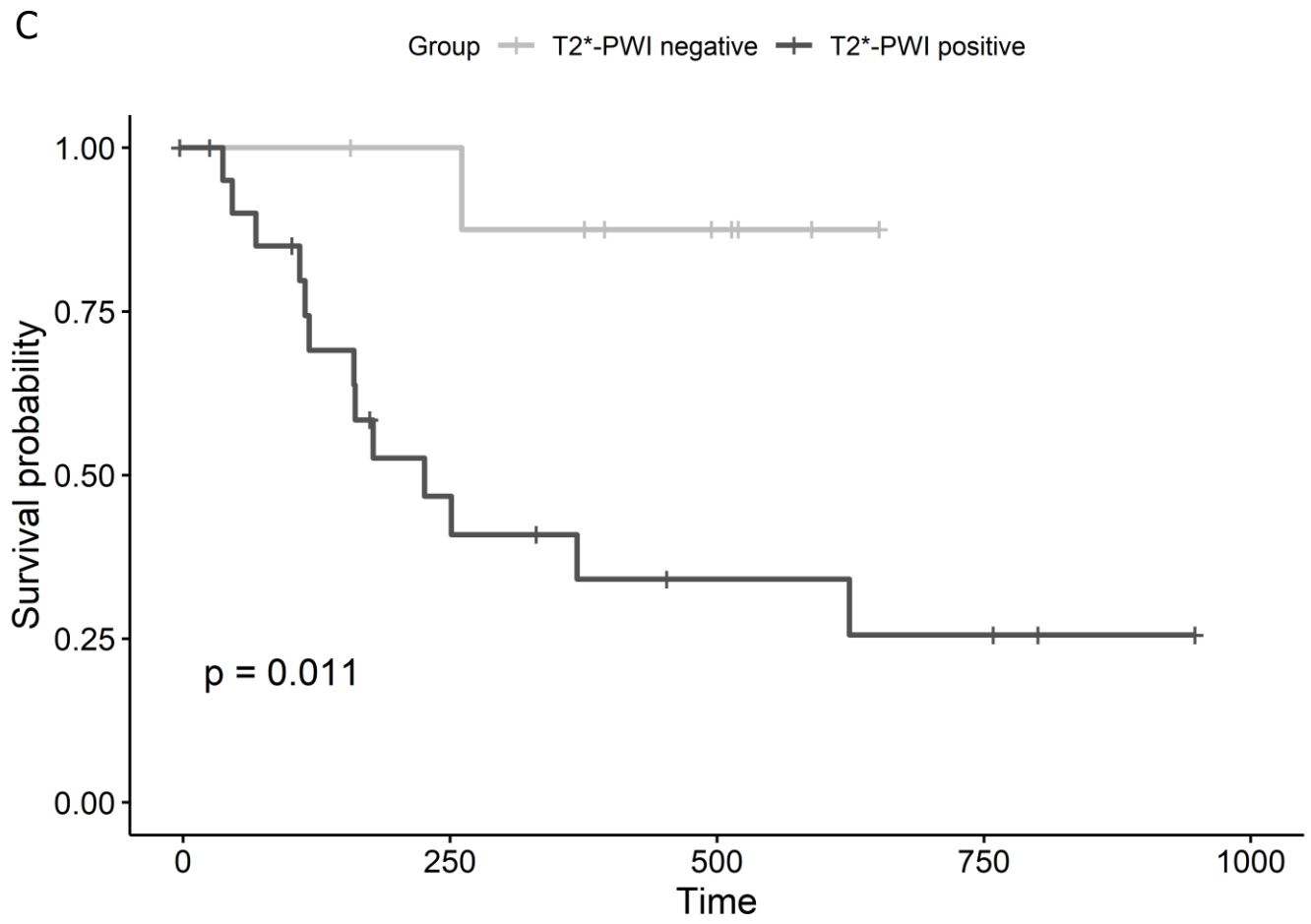

Supplemental FIG 6. Kaplan-Meier survival analysis of the patients with nonprogressed lesions versus progressed lesions (A), T1-PWI negative lesions versus positive lesions (B, T1-rCBV 90th percentile cutoff 4.930), and T2*-PWI negative lesions versus positive lesions (C, T2*-rCBV 90th percentile cutoff 4.453). The log-rank test showed significant difference between nonprogressed versus progressed lesions and T2*-PWI negative versus positive lesions, but not between T1-PWI negative versus positive lesions. This may be explained by the small number of T1-PWI negative group, owing to the high sensitivity (100%) but low specificity (57.1%) of the T1-PWI cutoff.

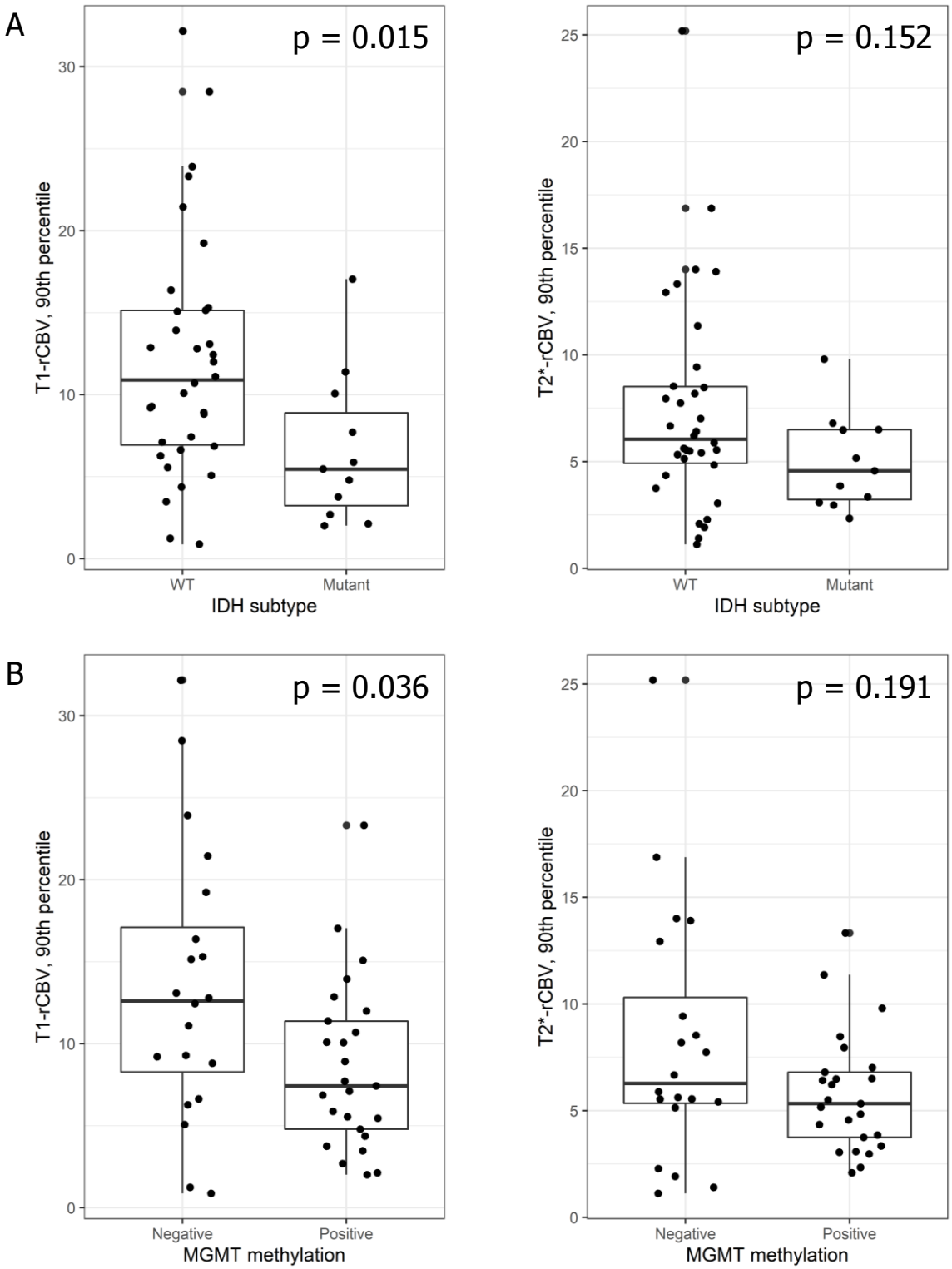

Supplemental FIG 7. Box plots displaying T1- and T2*-rCBV comparison between different genomic subclasses. The T1-rCBV values were significantly different between IDH-wildtype and IDH-mutant subgroups, but T2*-rCBV did not show significant difference between the same subgroups (A). Same results were shown between MGMT unmethylated and methylated subgroups (B).